Electronic Supplementary Material (ESI) for New Journal of Chemistry

Supplementary data:

Acridine-based enantioselective fluorescent sensors for malate anion in water

Kuo-Xi Xu, [a] Hua-Jie Kong,[a] Ping Li,[a] Li Yang,[a] Jing-Lai Zhang,[a] and Chao-Jie Wang[b]

Table of contents:

1. Copies of HRMS, ^{1}H and ^{13}C NMR spectra of sensors **S-/R-1, S-2** and **S-3**. 2-4
2. Binding experiments 5-11
3. Computational details 11-13

HRMS of compound **S-/R-1.**

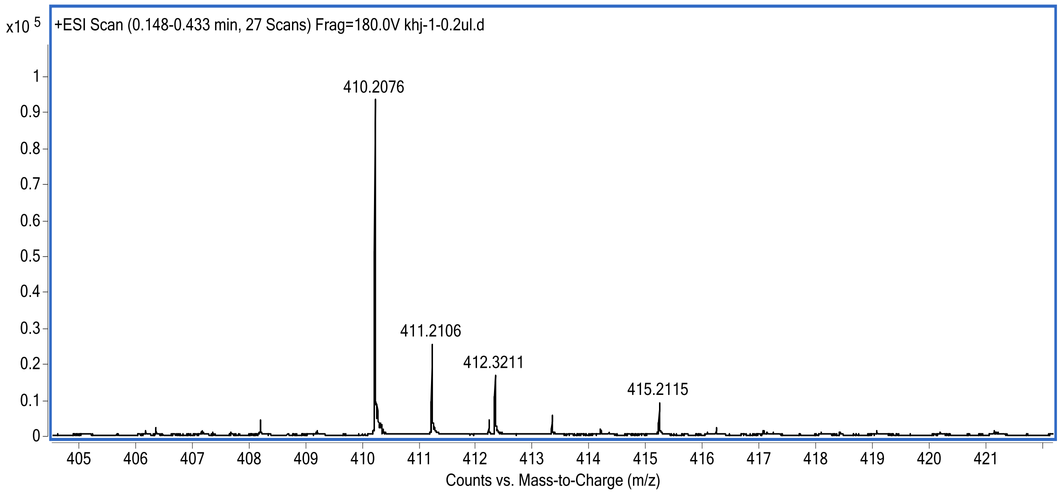

^{1}H and ^{13}C NMR spectra of compound **S-/R-1**.

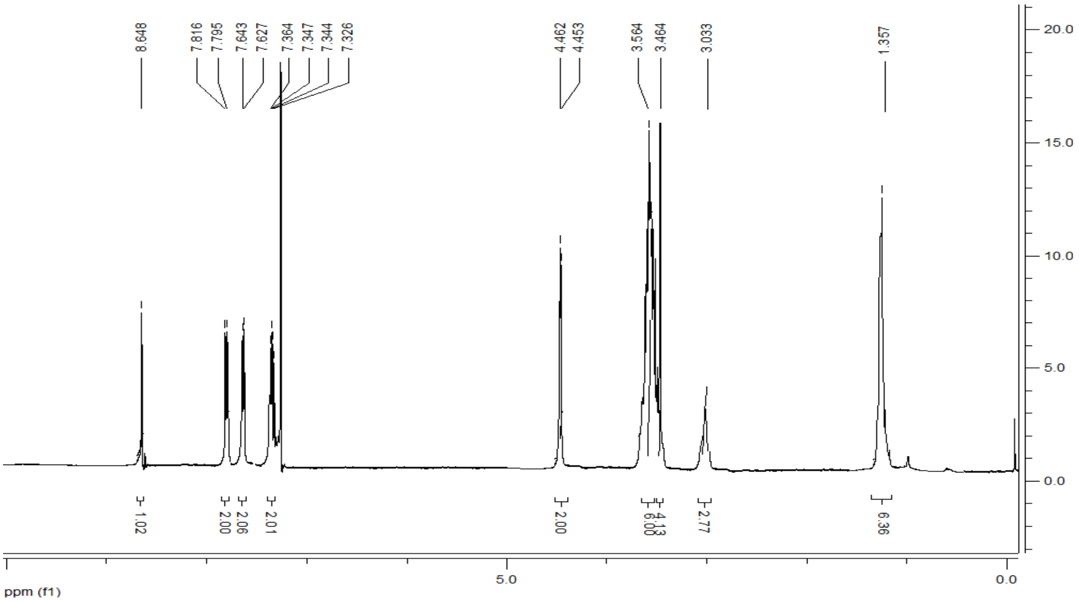

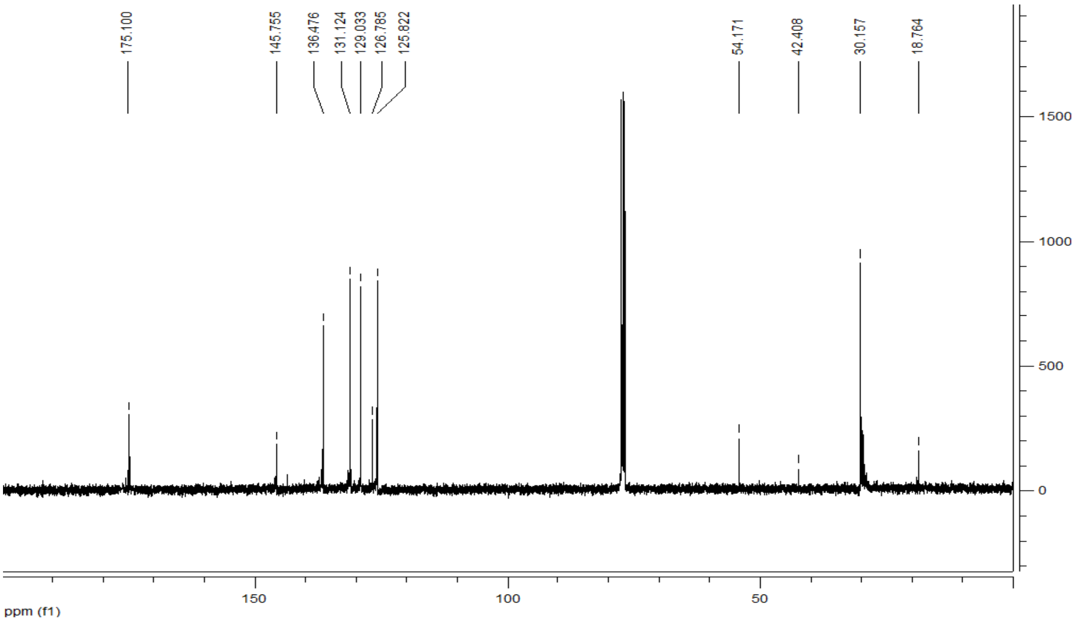

HRMS of compound **S-2.**

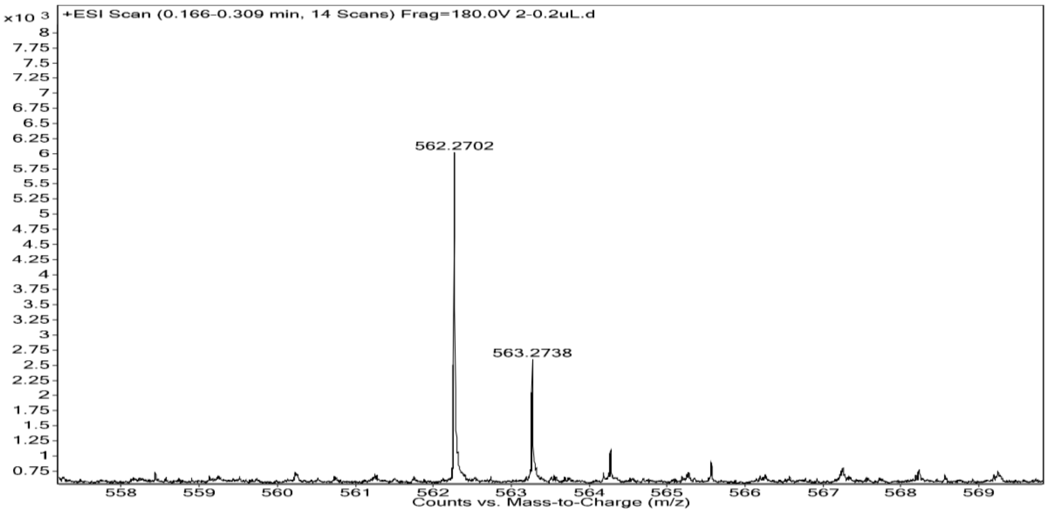

^{1}H and ^{13}C NMR spectra of sensor **S-2**.

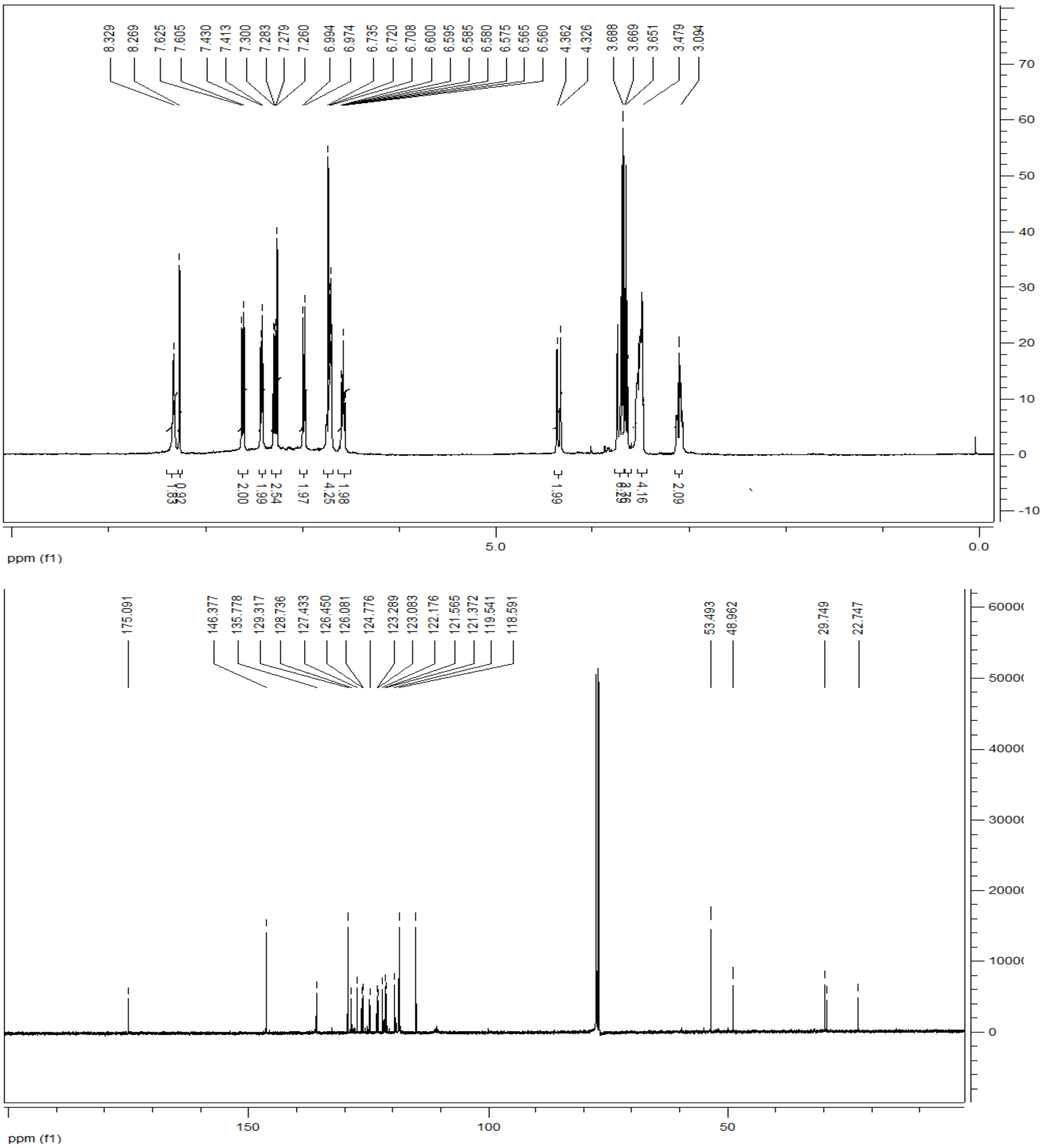

HRMS of compound **S-3.**

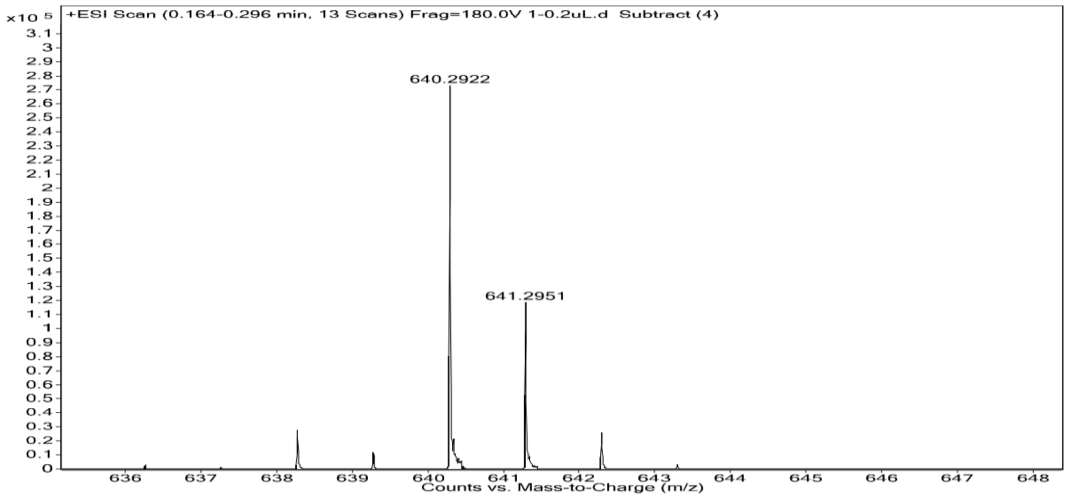

^{1} H and ^{13}C NMR spectra of sensor **S-3**.

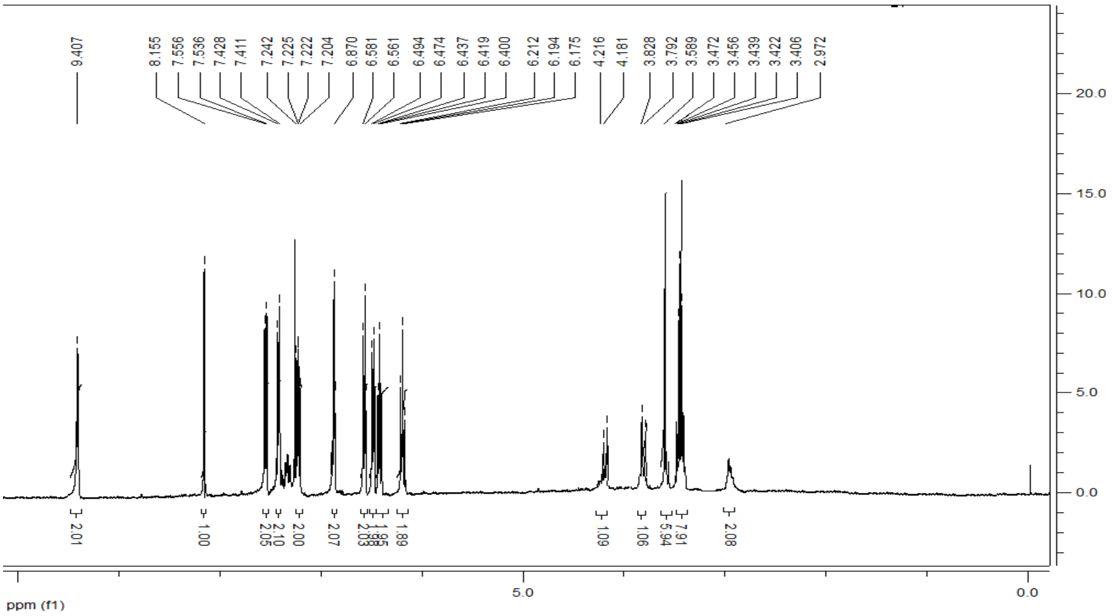

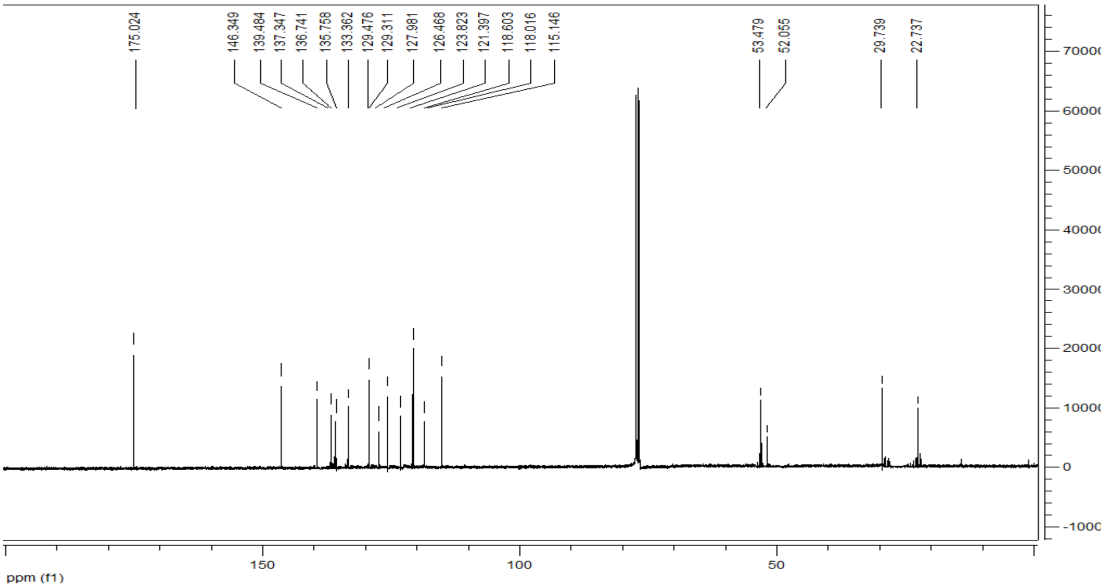

2. Binding experiments.

The sensor **S-1**:

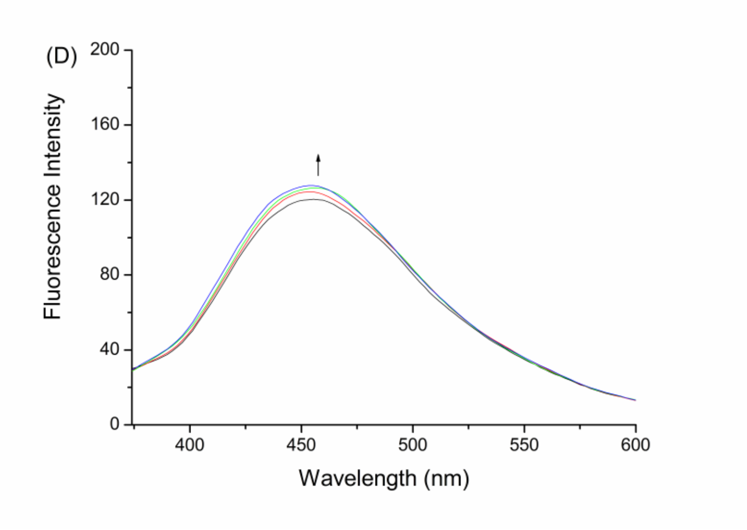

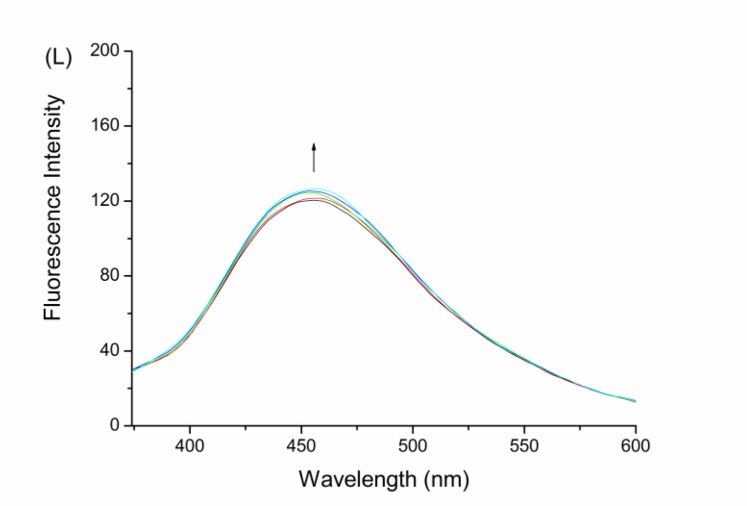

Fig. s1 Fluorescence spectra of sensor **S-1** (3.0×10^{-5} mol L^{-1}) upon addition of various amounts of *D*- or *L*-methoxyphenylacetic acid anion in H_2O (including 0.3%DMSO, 0.01 M HEPES buffer, pH 7.4). The equivalents of anion are: 0→97. λ_{ex}= 356 nm.

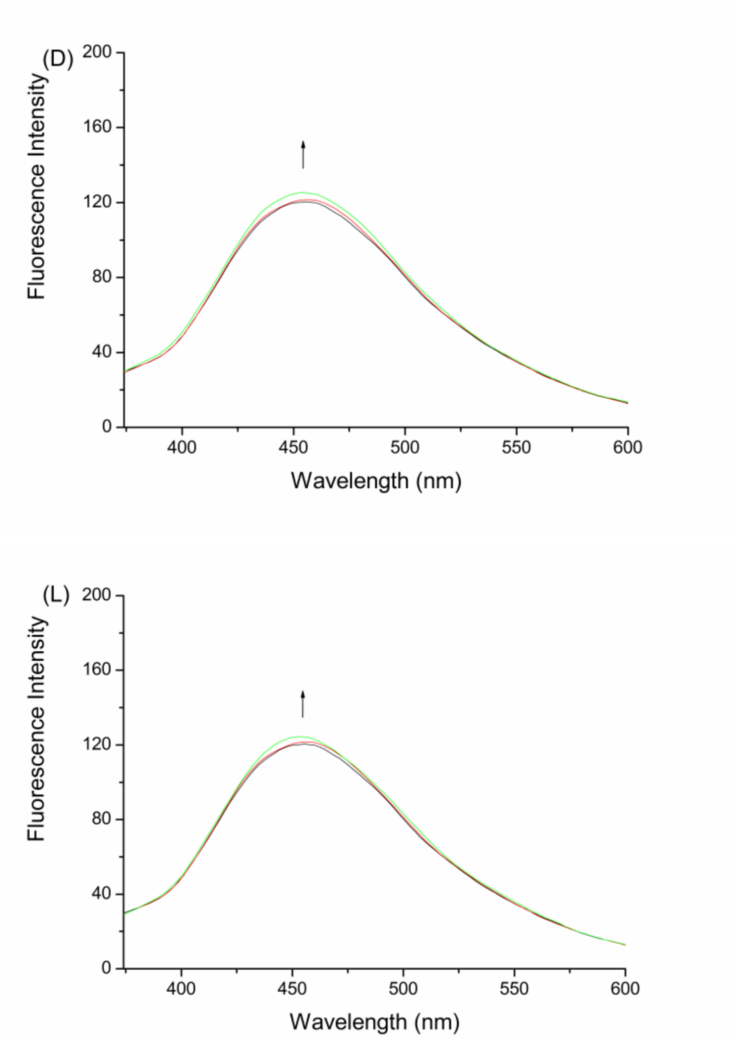

Fig. s2 Fluorescence spectra of sensor **S-1** (3.0×10^{-5} M) with *D*- or *L*-phenylalanine acid anion in buffered H_2O (including 0.3％DMSO, 0.01 M HEPES buffer, pH=7.4). Equivalents of anion: 0→97. λ_{ex}=356 nm (EX: 10; EM: 10).

The sensor **S-2**:

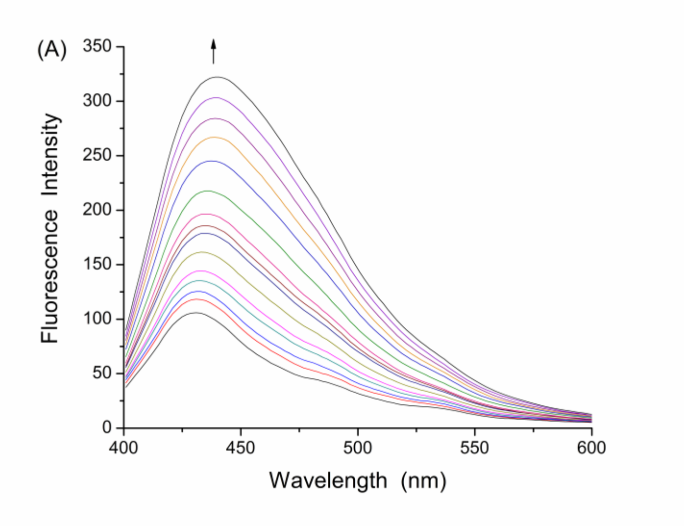

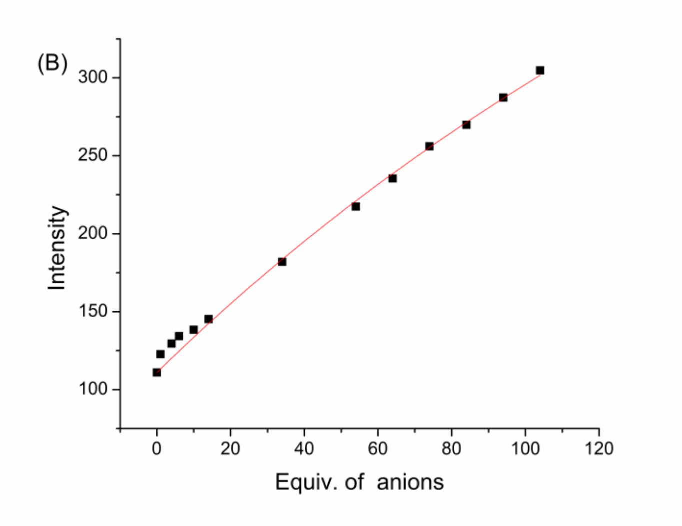

Fig. s3 (A): Fluorescence spectra of sensor **S-2** (3.0 ×10^{-5} M) with *D*-MA in buffered H_2O (including 0.3％DMSO, 0.01 M HEPES buffer, pH=7.4). Equivalents of anion: 0→104. λ_{ex}=371 nm (EX: 10; EM: 10). (B): changes in the fluorescence intensity of **S-2** at 438 nm upon addition of *D*-MA. The line shown is a line-fitted curve. The correlation coefficient (R) of the non-linear curve fitting is 0.9972.

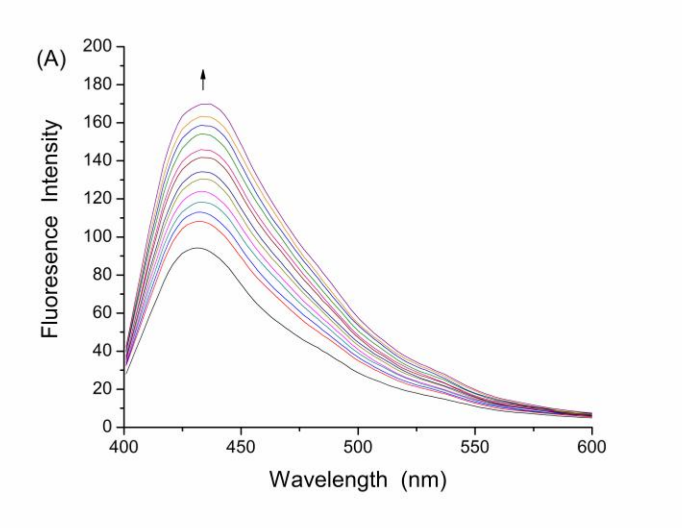

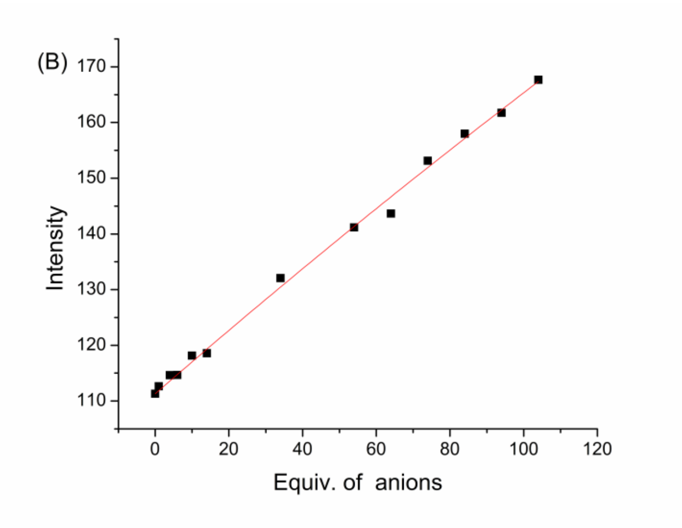

Fig. s4 (A): Fluorescence spectra of sensor **S-2** (3.0 ×10^{-5} M) with *L*-MA in buffered H_2O (including 0.3％DMSO, 0.01 M HEPES buffer, pH=7.4). Equivalents of anion: 0→104. λ_{ex}=371 nm (EX: 10; EM: 10). (B): changes in the fluorescence intensity of **S-2** at 438 nm upon addition of *L*-MA. The line shown is a line-fitted curve. The correlation coefficient (R) of the non-linear curve fitting is 0.9983.

The sensor **S-3**:

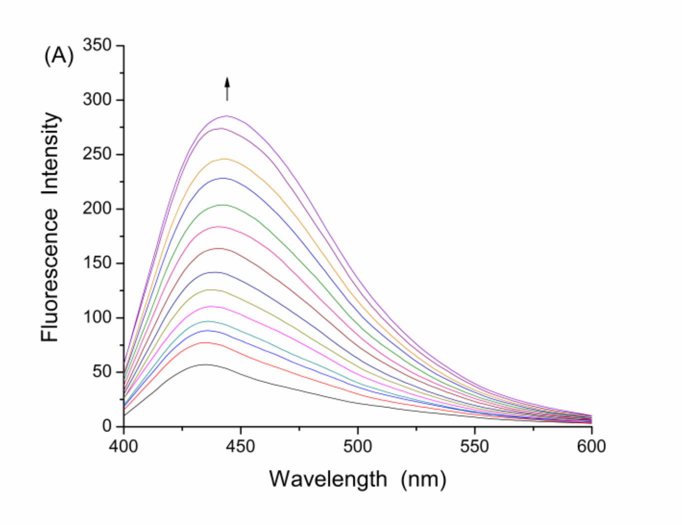

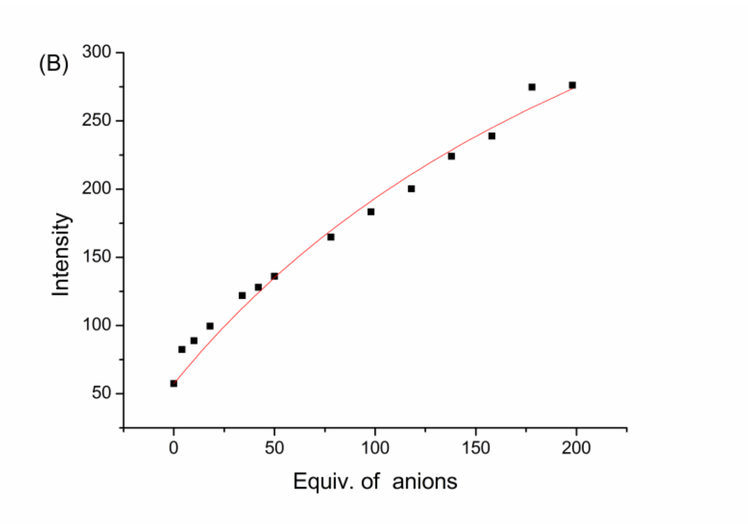

Fig. s5 (A): Fluorescence spectra of sensor **S-3** (3.0×10^{-5} M) with *D*-MA in buffered H_2O (including 0.3％DMSO, 0.01 M HEPES buffer, pH=7.4). Equivalents of anion: 0→198. λ_{ex}=376 nm (EX: 10; EM: 10). (B): changes in the fluorescence intensity of **S-3** at 438 nm upon addition of *D*-MA. The line shown is a line-fitted curve. The correlation coefficient (R) of the non-linear curve fitting is 0.9908.

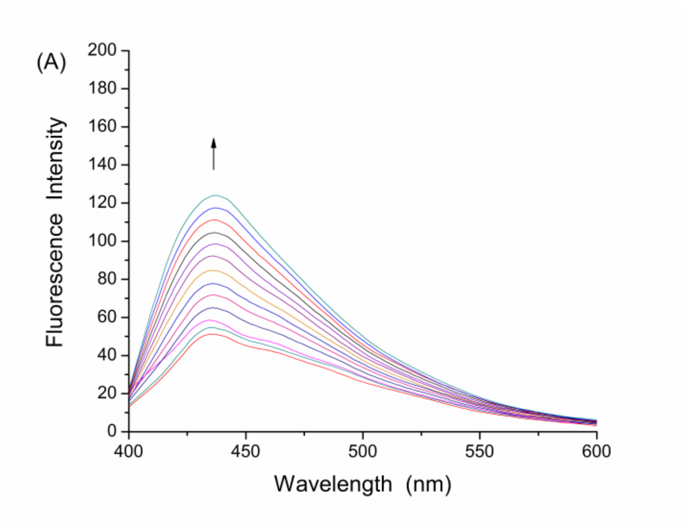

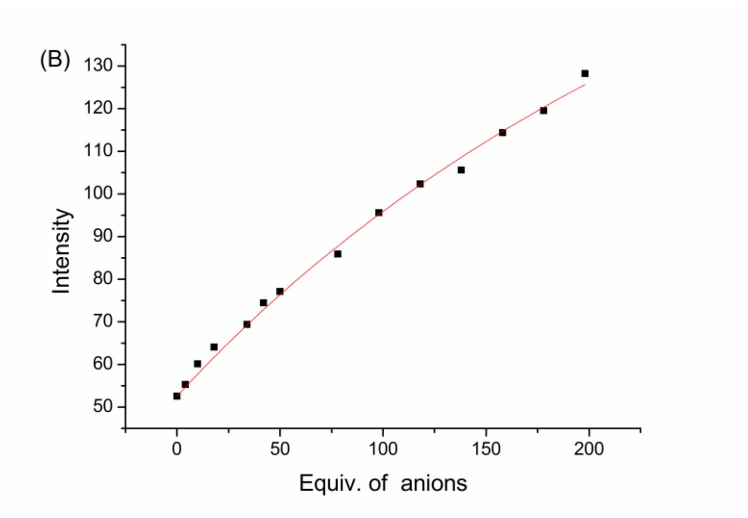

Fig. s6 (A): Fluorescence spectra of sensor **S-3** (3.0×10^{-5} M) with *L*-MA in buffered H_2O (including 0.3％DMSO, 0.01 M HEPES buffer, pH=7.4). Equivalents of anion: 0→198. λ_{ex}=376 nm (EX: 10; EM: 10). (B): changes in the fluorescence intensity of **S-3** at 438 nm upon addition of *L*-MA. The line shown is a line-fitted curve. The correlation coefficient (R) of the non-linear curve fitting is 0.9978.

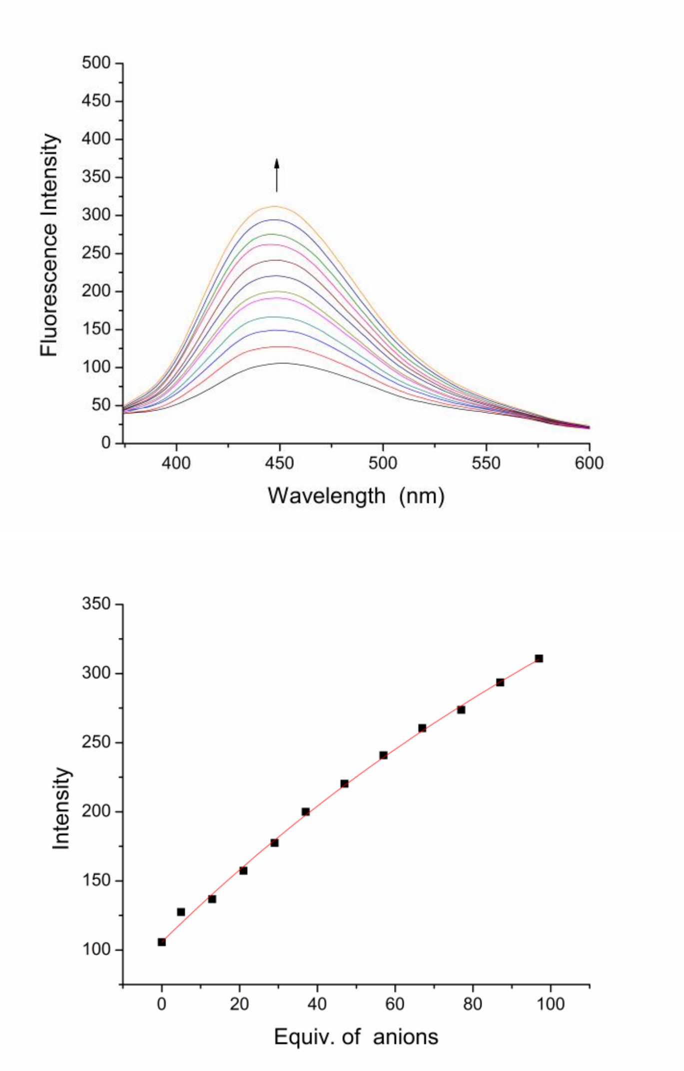

Fig. s7 (A): Fluorescence spectra of sensor **R-1** (3.0×10^{-5} M) with *L*-MA in buffered H_2O. Equivalents of anion: 0→97. λ_{ex}=356 nm (EX: 5; EM: 10). (B): changes in the fluorescence intensity of **R-1** at 450 nm upon addition of *L*-MA. The line shown is a line-fitted curve. The correlation coefficient (R) of the non-linear curve fitting is 0.9989.

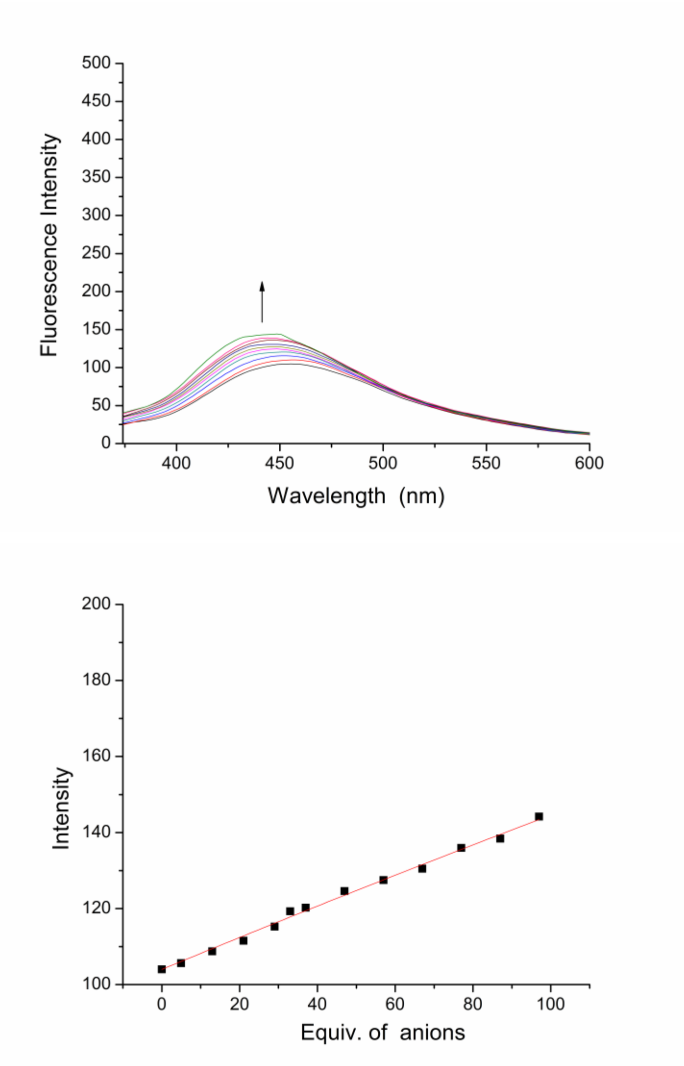

Fig. s8 (A): Fluorescence spectra of sensor **R-1** (3.0×10^{-5} M) with *D*-MA in buffered H_2O. Equivalents of anion: 0→97. λ_{ex}=356 nm (EX: 5; EM: 10). (B): changes in the fluorescence intensity of **R-1** at 450 nm upon addition of *D*-MA. The line shown is a line-fitted curve. The correlation coefficient (R) of the non-linear curve fitting is 0.9974.

Computational Details

The gaussion 03 series of programs used for all calculaions, [1] molecules were also fully structurally optimized at the B3LYP/6-31G(d, p) level of theory, the complex single point energy corrected by using the basis set superposition error(BSSE) at the B3LYP/6-31G(d, p) level of theory.

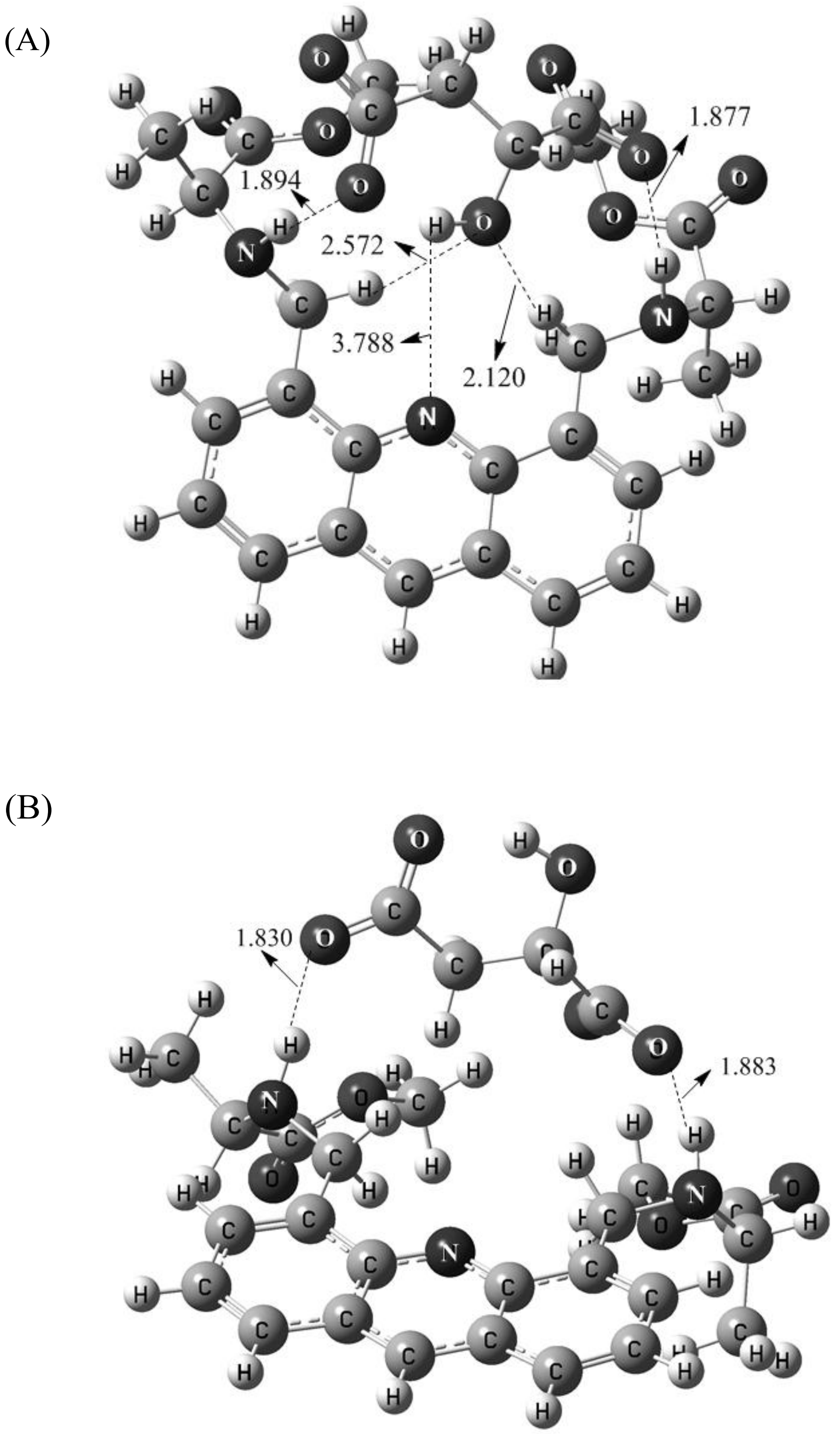

Fig. s9 (A) The mode of proposed 1:1 complexation of sensor **S-1**+*D*-MA; (B) The modes of proposed 1:1 complexation of sensor **S-1**+*L*-MA.

Table S1. Optimized Cartesian coordinates (Å) and energies (Hartree) of complex corrected by using the basis set superposition error(BSSE) at the B3LYP/6-31G(d, p) level of theory.

bond	Modle A	Modle B
	length (Å)	length (Å)
1C-2C	1.37584	1.37337

1C-6C	1.42175	1.42479
1C-14H	1.08603	1.08606
2C-3C	1.44411	1.4432
2C-22C	1.5248	1.51963
3C-4C	1.44902	1.4458
3C-21N	1.34314	1.34254
4C-5C	1.42608	1.42792
4C-7C	1.39762	1.39779
5C-6C	1.37066	1.37049
5C-15H	1.08925	1.089
6C-16H	1.08894	1.08874
7C-8C	1.39637	1.39826
7C-17H	1.09074	1.09057
8C-9C	1.44929	1.4476
8C-13C	1.42729	1.42722
9C-10C	1.44787	1.44572
9C-21N	1.3413	1.34145
10C-11C	1.37576	1.37471
10C-40C	1.52051	1.52174
11C-12C	1.42346	1.42429
11C-18H	1.08521	1.08514
12C-13C	1.36949	1.36982
12C-19H	1.08922	1.0888
13C-20H	1.0892	1.08899
22C-23H	1.09382	1.095
22C-24H	1.10168	1.10177
22C-25N	1.46464	1.45279
25N-26H	1.03234	1.04026
25N-27C	1.45003	2.66767
27C-29C	1.54101	1.54074
27C-28H	1.10178	1.10117
27C-33C	1.54295	1.54767
29C-30H	1.09826	1.09551
29C-31H	1.09616	1.09555
29C-32H	1.09624	1.09521
33C-34O	1.22218	1.22131
33C-35O	1.33338	1.333
350-36C	1.43993	1.44001
36C-37H	1.09398	1.09451
36C-38H	1.09579	1.09461
36C-39H	1.09498	1.09566
40C-41H	1.09969	1.09906
40C-42H	1.09858	1.09497
40C-43N	1.46664	1.46537

43N-44H	1.0312	1.02863
43N-45C	1.46132	1.46837
45C-46H	1.0978	1.09724
45C-47C	1.54131	1.54024
45C-54C	1.53823	1.53648
47C-48O	1.21809	1.21695
47C-49O	1.34109	1.34132
49O-50C	1.44313	1.44577
50C-51H	1.09431	1.09423
50C-52H	1.09266	1.09306
50C-53H	1.098	1.10141
54C-55H	1.09702	1.09708
54C-56H	1.09462	1.09443
54C-57H	1.09455	1.09394

E： Single point energy corrected by using the basis set superposition error (BSSE) at the B3LYP/6-31G(d, p) level of theory.
E1: the energy change of 1+*D*-MA is -204.1389262
E2：the energy change of 1+*L*-MA is -198.3504863

(1) Complete Ref. 1 of paper: Gaussian 09, Revision A.1, Frisch, M. J.; Trucks, G. W.; Schlegel, H. B.; Scuseria,G. E.; Robb, M. A.; Cheeseman, J. R.; Scalmani, G.; Barone, V.; Mennucci, B.; Petersson, G. A.; Nakatsuji, H.; Caricato, M.; Li, X.; Hratchian, H. P.; Izmaylov, A. F.; Bloino, J.; Zheng, G.; Sonnenberg, J. L.; Hada, M.; Ehara, M.; Toyota, K.; Fukuda, R.; Hasegawa, J.; Ishida, M.; Nakajima, T.; Honda, Y.; Kitao, O.; Nakai, H.; Vreven, T.; Montgomery, Jr. J. A.; Peralta, J. E.; Ogliaro, F.; Bearpark, M.; Heyd, J. J.; Brothers, E.; Kudin, K. N.; Staroverov, V. N.; Kobayashi, R.; Normand, J.; Raghavachari, K.; Rendell, A.; Burant, J. C.; Iyengar, S. S.; Tomasi, J.; Cossi, M.; Rega, N.; Millam, N. J.; Klene, M.; Knox, J. E.; Cross, J. B.; Bakken, V.; Adamo, C.; Jaramillo, J.; Gomperts, R.; Stratmann, R. E.; Yazyev, O.; Austin, A. J.; Cammi, R.; Pomelli, C.; Ochterski, J. W.; Martin, R. L.; Morokuma, K.; Zakrzewski, V. G.; Voth, G. A.; Salvador, P.; Dannenberg, J. J.; Dapprich, S.; Daniels, A. D.; Farkas, Ö.; Foresman, J. B.; Ortiz, J. V.; Cioslowski, J.; Fox, D. J. Gaussian, Inc., Wallingford CT, 2009.